BIOCHEMISTRY
including biophysical chemistry & molecular biology

Article

pubs.acs.org/biochemistry

Characterization of Sulfolipids of *Mycobacterium tuberculosis* H37Rv by Multiple-Stage Linear Ion-Trap High-Resolution Mass Spectrometry with Electrospray Ionization Reveals That the Family of Sulfolipid II Predominates

Elizabeth R. Rhoades,[†,§] Cassandra Streeter,[†] John Turk,[‡] and Fong-Fu Hsu*[,‡]

[†]Department of Microbiology and Immunology, C5 109 Vet Medical Center, Cornell University, Ithaca, New York 14853, United States

[‡]Mass Spectrometry Resource, Division of Endocrinology, Diabetes, Metabolism, and Lipid Research, Department of Internal Medicine, Box 8127, Washington University School of Medicine, St. Louis, Missouri 63110, United States

Supporting Information

ABSTRACT: *Mycobacterium tuberculosis*, the causative agent of tuberculosis, is unique among bacterial pathogens in that it contains a wide array of complex lipids and lipoglycans on its cell wall. Among them, the sulfated glycolipid, termed the sulfolipid, is thought to mediate specific host−pathogen interactions during infection. Sulfolipids (SLs), including sulfolipid I (SL-I) and sulfolipid II (SL-II), are 2,3,6,6′-tetraacyltrehalose 2′-sulfates. SL-I was identified as a family of homologous 2-palmitoyl(stearoyl)-3-phthioceranoyl-6,6′-bis-(hydroxyphthioceranoyl)trehalose 2′-sulfates and was believed to be the principal sulfolipid of *M. tuberculosis* strain H37Rv. We cultured and extracted sulfolipids using various conditions, including those originally described, and employed high-resolution multiple-stage linear ion-trap mass spectrometry with electrospray ionization to characterize the structure of the principal SL. We revealed that SL-II, a family of homologous 2-stearoyl(palmitoyl)-3,6,6′-tris(hydroxyphthioceranoyl)-trehalose 2′-sulfates, rather than SL-I is the principal sulfolipid class. We identified a great number of isomers resulting from permutation of the various hydroxyphthioceranoyl substituents at positions 6 and 6′ of the trehalose backbone for each of the SL-II species in the entire family. We redefined the structure of this important lipid family that was misassigned using the traditional methods 40 years ago.

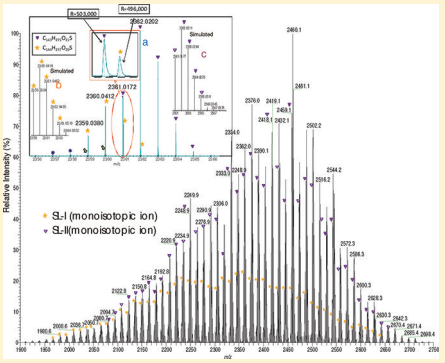

Mycobacterium tuberculosis contains a range of complex glycolipids with a trehalose backbone, including a family of sulfated acyl trehaloses that was first recognized by Middlebrook et al. in the virulent tubercle bacilli.[1] This family of sulfated acyl trehaloses defined as sulfolipids (SLs) was characterized by Goren and co-workers in their early studies of *M. tuberculosis* H37Rv.[2−5] The principal SLs were characterized as sulfolipid I (SL-I), which is a homologous mixture of 2,3,6,6′-tetraacyl-α,α′-D-trehalose 2′-sulfate consisting of a pair of 2,4,6,8,10,12,14,16-octamethyl-17-hydroxydotriacontanoates (hydroxyphthioceranoic acid) located at positions 6 and 6′, and a nonhydroxylated multiple-methyl-branched derivative (phthioceranoic acids) and a short saturated fatty acid (palmitic acid or stearic acid) located at positions 3 and 2 of the trehalose backbone, respectively. In addition to the major SL-I, minor species that were termed SL-II [2-palmitoyl/stearoyl-3,6,6′-tris(hydroxyphthioceranoyl)trehalose 2′-sulfate], SL-I′ [2-palmitoyl/stearoyl-3,6-bis(phthioceranoyl)-6′-hydroxyphthioceranoyltrehalose 2′-sulfate], and SL-II′ [2-palmitoyl/stearoyl-4,6,6′-tris(hydroxyphthioceranoyl)trehalose 2′-sulfate] were also reported. However, the structural studies of SLs have focused on SL-I.[4]

A wealth of in vivo and in vitro studies that point to the role of sulfolipids in the virulence of the tubercle bacillus have been conducted. For example, Okamoto et al. reported that SL could contribute to virulence at early stages of mycobacterial infection or stimulation with the glycolipids by counteracting the immunopotentiating effect of TDM.[6] In vitro, SL-I induced swelling and disruption of mitochondrial membranes and strongly inhibited mitochondrial oxidative phosphorylation.[7] *M. tuberculosis* sulfolipids are also capable of preventing phagosome−lysosome fusion in cultured macrophages.[8] From in vitro studies, Zhang and co-workers reported the remarkable properties of sulfolipids, including their ability to modulate the oxidative response and the cytokine secretion of human monocytes and neutrophils.[9,10] It was also found that diacylated sulfoglycolipids are mycobacterial antigens that can stimulate CD1-restricted T cells during infection with *M. tuberculosis*.[11−13] Studies addressing aspects of the biosynthesis and the function of SL-1 in vivo have recently begun to

Received: August 4, 2011
Revised: September 13, 2011
Published: September 15, 2011

emerge.[14−17] However, its function in the life cycle of *M. tuberculosis* remains largely unknown.

The structures of sulfolipids are complex, and studies of the structural definition of SL-I conducted by Goren and co-workers 40 years ago are showcases of the exceptional talent of scientists of their generation. They were able to deduce the complex structure of unknown compounds using the traditional methods that required many laborious steps to a large-scale separation and purification, followed by multiple chemical reaction steps and chromatographic separations, in conjunction with various spectroscopic techniques, including IR, NMR, and mass spectrometry for structure analysis.[2−4] In this work, we describe a simple and direct electrospray ionization (ESI) mass spectrometric approach employing multiple-stage and high-resolution mass spectrometry for structural elucidation of the sulfolipids of *M. tuberculosis* H37Rv, the same strain previously described by Goren et al.[2−5] When cells were cultured and extracted using various conditions, including those described by Goren, we found that SL-II, not SL-I, is always the principal sulfolipid class. Our data are similar to those reported by others who nevertheless referred to it as SL-I.[4,16,18−20] Our approaches using various mass spectrometric techniques permit us to reveal the detailed structures of SLs, including the various isobaric isomers that had been reported but not confirmed by the traditional methods.

EXPERIMENTAL PROCEDURES

Materials. Sulfolipid I standard (this standard, in fact, is mainly Sulfolipid II) was supplied by the Mycobacteria Research Laboratories at Colorado State University (CSU) as part of the TB Research materials contract that is currently administered by BEI Resources (http://www.beiresources.org/TBVTRMResearchMaterials/tabid/1431/Default.aspx). According to standard operating protocols, the SL-I standard was harvested from *M. tuberculosis* H37Rv that had been grown in glycerol−alanine−salts (GAS) broth, killed (γ-irradiation), and extracted using chloroform and methanol. All other chemicals used are spectroscopic grade and were purchased from Sigma Chemical Co.

Culture Media. Modified Wong−Weinzirl broth was prepared and autoclaved as described by Goren.[2] The broth consisted of malic acid (0.3%), NH_4OH (0.12%), ammonium citrate (0.5%), KH_2PO_4 (0.6%), anhydrous Na_2CO_3 (0.2%), NaCl (0.2%), $MgSO_4$ (0.1%), ammonium iron(III) citrate (0.005%), glycerol (0.05%, v/v), and glucose (0.2%), supplemented with sodium pyruvate (0.05%), Cu^{2+} (0.0001%), and Zn^{2+} (0.0001%). Middlebrook 7H9 broth and Middlebrook 7H10 plates (BD, Franklin Lakes, NJ) were prepared according to the manufacturer's instructions with supplemental OADC enrichment and Tween 80 (0.05%). GAS broth contained (per liter) 2 g of NH_4Cl, 1 g of L-alanine, 0.3 g of Bacto casitone (Difco), 4 g of K_2HPO_4, 2 g of citric acid, 50 mg of ferric ammonium citrate, 1.2 g of $MgCl_2{\cdot}6H_2O$, 0.6 g of K_2SO_4, 1.8 mL of 10 M NaOH, 10 mL of glycerol, and Tween 80 (0.05%).

Mycobacterial Culture and Harvest. Seed stocks of *M. tuberculosis* (H37Rv or CDC1551) were grown for 7−10 days (OD = 0.7−0.9) in 7H9-OAD at 37 °C. For broth-grown cultures, 250 mL of broth was inoculated (1:500) and incubated at 37 °C for 4−6 weeks to late-log phase. Pellicles formed in the modified Wong−Weinzirl broth, and flocculent cultures grew in 7H9 broth. Broth cultures were harvested by centrifugation at 3000 rpm, and the pellets were washed successively in a PBS/Tween (0.05%) mixture. For plate-grown cultures, seed cultures were diluted 1:10 in a PBS/Tween mixture and vortexed; and 4 mL was spread onto 7H10 agar (150 cm diameter plates) and incubated at 37 °C for 6 weeks. Confluent growth with a dry, waxy appearance was scraped into collection tubes and weighed.

Lipid Extraction. Pellets of live bacilli were extracted in a hexane/decylamine or chloroform/methanol (C/M) (2:1, v/v) mixture. Plate-grown pellets were extracted three times (100 mL of solvent per 100 g). Hexane/decylamine extractions were performed as described by Goren.[2] Briefly, the first extraction was conducted in 0.1% decylamine (4 °C for 1−4 weeks), and the subsequent extractions were conducted in 0.5% decylamine with sonication for 30 min at room temperature. For C/M extractions, washed pellets were extracted the first time at 4 °C for 1−4 weeks and subsequently with sonication for 30 min at room temperature. Extracts were pooled, filtered (0.2 μm, PFTE filters), and dried on a rotary evaporator. To remove decylamine, residues were dissolved in hexane, and an equal volume of citric acid (1 N) was added. The flask was shaken, and the contents were allowed to separate. The top phase was percolated through a column (8 cm length, 0.7 cm diameter) of anhydrous H_2SO_4 and chased with 1 column volume of hexane. The eluent was dried under nitrogen. All crude extracts were stored dried and under nitrogen at −70 °C.

Thin Layer Chromatography. Lipid extracts were dissolved in hexane. If a sample was insoluble, a chloroform/methanol (2:1) mixture was added until the sample dissolved completely. Lipids were spotted onto silica gel 60 TLC plates (EM Science) and developed in a two-solvent system as previously reported by Goren et al.[2] Plates were developed first in a chloroform/methanol/acetic acid/water (95:1:5:0.3, v/v) solvent to 20 cm, dried, and then redeveloped in a chloroform/acetone/methanol/water/acetic acid (158:83:1:6:32, v/v) solvent to 15 cm. Plates were sprayed with ethanolic sulfuric acid (50%) and charred with a heat gun. Samples that were fractionated by preparative TLC were loaded across a TLC plates and developed successively in the same solvent systems for 20 and 18 cm, respectively. A strip of the plate was charred to visualize lipid bands, and the corresponding areas were scraped into separate tubes and extracted from the silica with hexane followed by a chloroform/methanol (2:1) mixture, each for 5 min at 45 °C with sonication. The two extracts were combined, dried under nitrogen, and stored at −70 °C.

Mass Spectrometry. Low-energy collision-induced dissociation (CID) tandem mass spectrometry experiments were conducted on a Thermo Scientific (San Jose, CA) LTQ Orbitrap Velos and LIT-FT mass spectrometers with the Xcalibur operating system. High-resolution mass spectrometry was also performed on a Bruker (Bremen, Germany) *solariX* 12 T FTMS system, which provides baseline resolution among ions from SL-I and SL-II. A solution of sulfolipid in methanol was infused (1.5 μL/min) to the ESI source, where the skimmer was set at the ground potential, the electrospray needle was set at 4.0 kV, and the temperature of the heated capillary was 300 °C. The automatic gain control of the ion trap was set to 5×10^4, with a maximum injection time of 100 ms. Helium was used as the buffer and collision gas at a pressure of 1×10^{-3} mbar (0.75 mTorr). The MS^n experiments were conducted with an optimized relative collision energy ranging from 35 to 40%, an activation q value of 0.25, and an activation time of 10 ms to leave a minimal residual abundance of precursor ion (~20%). The mass selection window for the

precursor ions was set at 4 Da wide to include the monoisotopic species to the ion trap for collision-induced dissociation. For higher-energy collision-induced dissociation (HCD), precursor ions were selected in the linear ion trap and via fragmentation in the multipole HCD collision cell with high-resolution accurate mass detection in the Orbitrap mass analyzer. Mass spectra were recorded in the profile mode, typically for 3−10 min for MS^n spectra (n = 2, 3, or 4).

Nomenclature. To facilitate the interpretation of data, the following abbreviations were adopted. The nonhydroxylated multiple-methyl-branched phthioceranoic acids, for example, the 2,4,6,8,10,12,14,16-octamethyldotriacontanoic acid, are designated as C_{40}-acids to reflect the fact that the structure consists of 40 saturated hydrocarbon chains. For hydroxydotriacontanoic acids, for example, 2,4,6,8,10,12,14,16-octamethyl-17-hydroxydotriacontanoic acid is designated as hC_{40}-acid to reflect the fact that the compound consists of 40 hydrocarbon chains with one hydroxyl group attached at C-17. Therefore, the principal SL-II species (the position of the substituents on the trehalose backbone is adopted from the definition of Goren[4]), which is a 2-stearoyl-3,6′-tris(2,4,6,8,10,12,14,16-octamethyl-17-hydroxydotriacontanoyl)-α,α'-D-trehalose 2′-sulfate, is designated as [18:0,hC_{40},hC_{40},hC_{40}]-SL, signifying that the compound consists of one stearoyl and three 2,4,6,8,10,12,14,16-octamethyl-17-hydroxydotriacontanoyl groups located at positions 2, 3, 6, and 6′ of the trehalose backbone, respectively, while an SL-I molecule such as 2-palmitoyl-3-2,4,6,8,10-pentamethyl-pentaeicosanoyl-6,6′-bis-(2,4,6,8,10,12,14,16-octamethyl-17-hydroxydotriacontanoyl)-α,α'-D-trehalose 2′-sulfate is designated as [16:0,C_{30},hC_{40},hC_{40}]-SL.

RESULTS AND DISCUSSION

Crude Sulfolipid Extracts from Different Culture Media and Extraction Methods. Various culture media and extraction methods have been used in reports characterizing the SLs from *M. tuberculosis* H37Rv.[2,11,16,19] To determine whether such variables could alter the relative abundance of the major SL families, H37Rv was cultured to late-log phase in four culture media, and two extraction methods were used. H37Rv and a clinical isolate [CDC1551 (data not shown)] yielded relatively abundant SLs in crude lipid extracts under all conditions (Figure 1). Glycolipids appeared as prominent red spots or streak on TLC plates when they were sprayed with sulfuric acid and heated, and spots with approximate R_f values of 0.44 and 0.49 that were scraped from prepTLC plates were confirmed to be SLs by ESI mass spectrometry in the negative-ion mode. The most abundant SL exhibited an R_f of 0.44 with a mobility identical to that of members of the SL-I family and a less abundant SL (R_f = 0.49), which was apparent in hexane/decylamine extracts, corresponding to the SL family that was designated SL-II by Goren.[2,4]

Sulfolipids from plate-grown cultures were especially abundant. SLs were also readily extracted from broth-grown cultures despite some culture-to-culture variation in the amounts of crude lipid (Figure 1, lanes 5 and 9 vs lane 6). The SLs that migrated at an R_f of 0.44 were always the most abundant SL family in all broth cultures. Hexane/decylamine or chloroform/methanol extraction methods isolated the major SL family; however, hexane/decylamine extraction was more efficient for isolating the SLs that migrated at an R_f of 0.49, as described by Goren.[2] Another parameter that was explored briefly was whether live and dead bacterial pellets yielded the same relative abundance of SL families. Preliminary studies showed no significant differences in crude extracts from heat-killed (autoclaved) versuss live bacterial pellets. Taken together, these data indicate that the SL family with an R_f of 0.44 in our TLC system is the most abundant family, irrespective of differences in commonly used culture media and extraction methods.

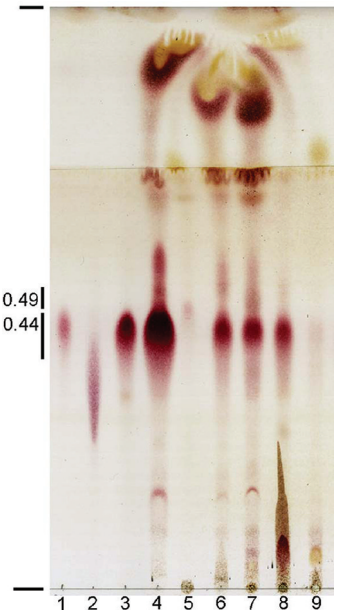

Figure 1. TLC comparison of crude lipid extracts from *M. tuberculosis* H37Rv. Purified standards or crude lipids that were obtained under various conditions were spotted and developed in two solvents in the same direction. Standards, samples, and the conditions under which they were obtained (if known) are indicated: lane 1, SL-I standard from the CSU TB materials research contract (GAS broth, C/M extraction); lane 2, trehalose dimycolate standard from Sigma-Aldrich; lane 3, purified major SL (GAS broth, C/M extraction); lane 4, crude lipids (7H10 plates, H/D extraction); lanes 5 and 6, crude lipids from different cultures (7H9 broth, HD extraction); lane 7, crude lipids (Wong−Weinzirl broth, HD extraction); lane 8, crude lipids (7H10 plates, C/M extraction); and lane 9, crude lipids (7H9 broth, C/M extraction). The average R_f values of the SL families are indicated as well as the origin and the most distant solvent front.

High-Resolution Mass Spectrometry of the $[M - H]^-$ Ions of Sulfolipids. We examined the SLs isolated from *M. tuberculosis* strain H37Rv and strain CDC1551 grown in 7H9 broth, and in modified Wong−Weinzirl broth, together with the sulfolipid standard obtained from the Mycobacterial Research Laboratories at CSU using ESI mass spectrometry in the negative-ion mode. An array of $[M - H]^-$ ions in the range of 2000−2900 Da, with an intermittence of 14 Da, was observed. The ESI/MS profiles of the SLs from H37Rv grown in 7H9 broth (Figure 2) and from the SL standard (not shown) are similar, and the profiles are also similar to those previously reported.[16,18−21] The SL profiles from strain H37Rv grown in modified Wong−Weinzirl broth (see Figure S1 of the Supporting Information) are also similar, and the ions representing SL-II are the dominant species; however, the average molecular mass is 56 Da higher than that obtained from 7H9 broth. The results indicate that the length of the hydroxyphthioceranoic acid substituents of SLs is dependent on the growth conditions. High-resolution mass spectrometric analysis on the ion series with an increment of 14 Da using an

dx.doi.org/10.1021/bi2012178|*Biochemistry* 2011, 50, 9135−9147

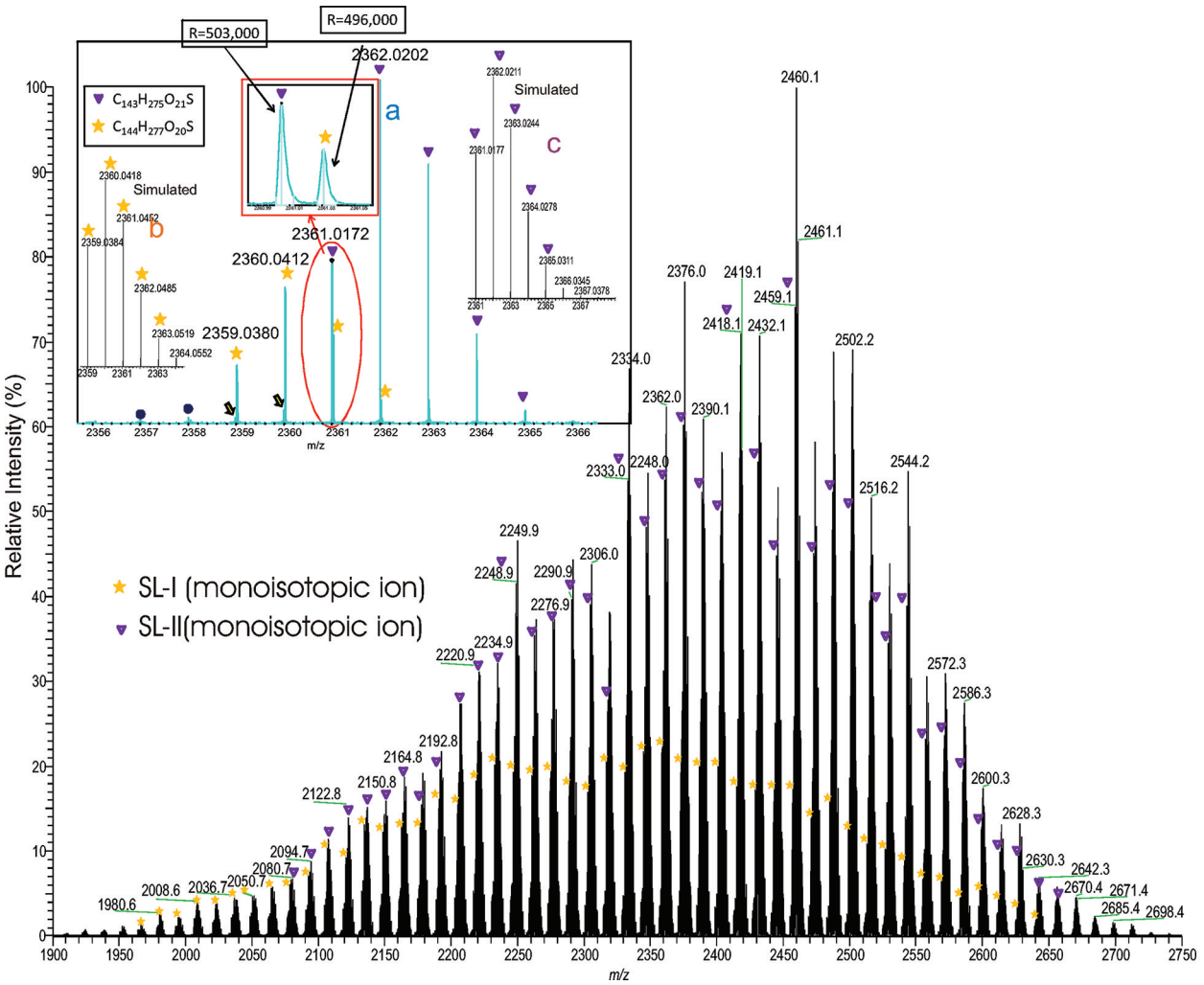

Figure 2. High-resolution ESI-MS spectrum of the $[M - H]^-$ ions of sulfolipids of H37Rv grown in Middlebrook 7H9 broth. The spectrum was obtained with a FTICR instrument. The high-resolution (resolution of 500000) readily separated the SL-I (monoisotopic ions labeled with ∗) class from the SL-II (monoisotopic ions labeled with ▼) class, which is the principal sulfolipid class from *M. tuberculosis* strain H37Rv (inset). The elemental compositions deduced from accurate mass measurements also define SL-I and SL-II.

FT-ICR instrument (resolution of ~500000) confirmed that the 14 Da increment corresponds to a CH_2 residue and the homologous $[M - H]^-$ ions that ranged from 1900 to 2750 Da all possess a $C_{120}H_{229}(CH_2)_nO_{21}S_1$ (n = 0, 1, 2, ..., 60) elemental composition (see Table S1 of the Supporting Information), in which the nominal masses for the monoisotopic peaks at m/z 2333, 2375, 2417, 2459, ..., 2501 are among the most prominent (Figure 2, ions labeled with ▼). This ion series consists of palmitoyl/stearoyl, three hydroxyphthioceranoyl, and one sulfate residue on the trehalose backbone and was previously defined as SL-II by Goren and coworkers.[4] The spectrum also contained the ion series with nominal monoisotopic masses that are 2 Da lighter (see Figure 2, ions labeled with ∗), similar to that recently reported by Layre et al.[21] High-resolution mass measurements on these ions (Table S1 of the Supporting Information) indicate that these ions have a $C_{120}H_{229}(CH_2)_nO_{20}S_1$ (n = 0, 1, 2, ..., 60) elemental composition, corresponding to the SL-I structures previously defined.[4]

The separation of the ion clusters of SL-I from those of SL-II (Figure 2, inset a) also provides an accurate profile of the isotopic cluster ions for confirmation of the elemental composition. For example, the monoisotopic ion observed at m/z 2359.0380 (Figure 2, inset a) corresponds to a $C_{144}H_{277}O_{20}S$ elemental composition (calculated mass of m/z 2359.0384), which gave a simulated spectrum (inset b, ions labeled with ∗) similar to the experimental spectrum (inset a, ions labeled with ∗). The monoisotopic ion observed at m/z 2361.0172 and its isotopic ion cluster pattern (inset a, ions labeled with ▼) are also consistent with a $C_{143}H_{275}O_{21}S$ elemental composition (calculated mass of m/z 2361.0177; the simulated plot of the isotopic ion clusters is labeled with ▼ in inset c), indicating the presence of SL-II. The mass spectrometric approaches to structural characterization of the major sulfolipid species (i.e., SL-II) are described below.

Structural Analysis of SL-II by Multiple-Stage Mass Spectrometry in Conjunction with High-Resolution Accurate Mass Measurements. High-resolution mass measurement of the $[M - H]^-$ ion of the monoisotopic ion at m/z 2459 (base peak) and its isotope ion cluster profile led to a $C_{150}H_{289}O_{21}S_1$ elemental composition (calculated mass of m/z 2459.1272, measured mass of m/z 2459.1272), corresponding to an SL-II molecule (Table S1 of the Supporting Information and Figure 2).

The MS^2 spectra of the ions at m/z 2459.1 following CID (Figure 3a) and HCD (Figure 3b) yielded a prominent ion at

dx.doi.org/10.1021/bi2012178|*Biochemistry* 2011, 50, 9135–9147

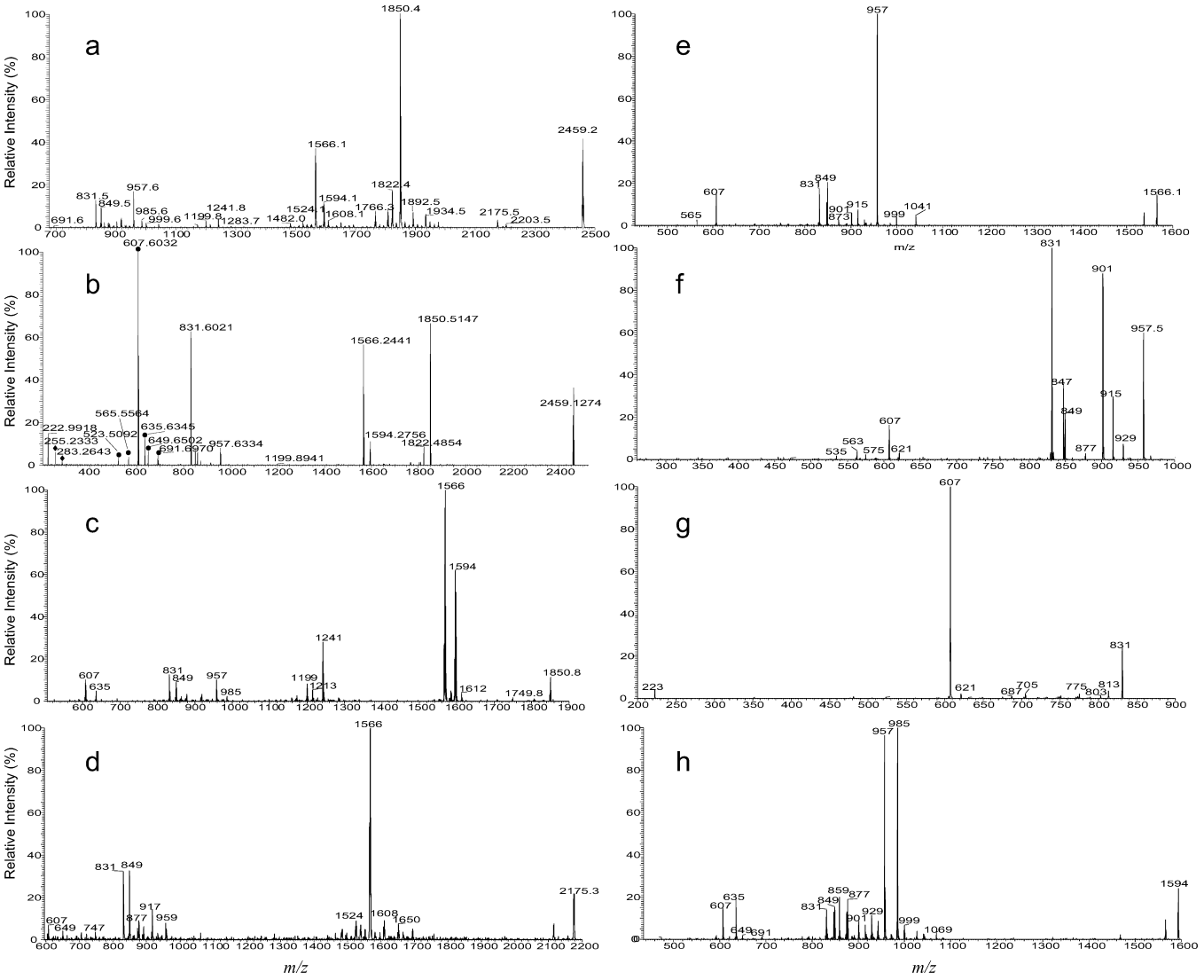

Figure 3. LIT CID MS^2 spectrum (a) and high-resolution HCD MS^2 spectrum (b) of the ion at m/z 2459. The low-mass fragment ions from HCD MS^2 (b) readily identify the hydroxyphthioceranoic acid (●), long chain fatty acid (◆), and sulfate groups (seen at m/z 222.9918), while the LIT CID MS^3 spectra of m/z 1850 (m/z 2459 → m/z 1850) (c), m/z 2178 (m/z 2459 → m/z 2178) (d), and m/z 1566 (m/z 2459 → m/z 1566) (e) and MS^4 spectra of m/z 957 (m/z 2459 → m/z 1566 → m/z 957) (f) and m/z 831 (m/z 2459 → m/z 1566 → m/z 831) (g) together with the MS^3 spectrum of m/z 1594 (m/z 2459 → m/z 1594) (h) support the fragmentation processes as illustrated in Scheme 1.

m/z 1850.6 (m/z 2459.1 − m/z 608.6), corresponding to the loss of a C_{40}-hydroxyphthioceranoic acid residue probably residing at position 3 of the trehalose core of the SL. The spectra also contained an abundant ion at m/z 1566.3 from further loss of a stearic acid (18:0-acid) residue at position 2 of the trehalose skeleton. This consecutive loss of the 18:0-fatty acid is supported by the CID MS^3 spectrum of the ion at m/z 1850 [m/z 2459.1 → m/z 1850.6 (Figure 3c)], which is dominated by the ion at m/z 1566.3 (m/z 1850.6 − m/z 284.3). The ion at m/z 1566.3 can also arise from the primary loss of the 18:0-fatty acid, followed by loss of a C_{40}-hydroxyphthioceranoic acid. These fragmentation processes were supported by the observation of the ion at m/z 1566.3 in the MS^3 spectrum of the ion at m/z 2174.8 [m/z 2459.1 → m/z 2174.8 (Figure 3d)] and consistent with the presence of the ion at m/z 2174.8 (m/z 2459.1 − m/z 284.3) in Figure 3a. The prominence of the ions at m/z 1850 and 1566 (Figure 3a,b) may indicate the preferential losses of the 3-acyl and 2-acyl substituents as the free fatty acid over those located at position 6 or 6′ and is consistent with the notion of the greater stability of the substituent at position 6 (or 6′) toward acid or alkaline hydrolysis as compared with those located at positions 2 and 3.[5] The MS^4 spectrum of the ion at m/z 1566.3 [m/z 2459.1 → m/z 1850.3 → m/z 1566.3 (Figure 3e)] is identical to the MS^3 spectrum of the ion at m/z 1566.3 (m/z 2459.1 → m/z 1566.3) (not shown), and the spectrum is dominated by the ion at m/z 957.7 (m/z 1566.3 − m/z 608.6), arising from the further loss of a C_{40}-hydroxyphthioceranoic acid residue, residing at position 6 or 6′. The spectrum also contained the ions at m/z 849.5 and 831.5, corresponding to 6′-C_{40}-hydroxyphthioceranoylglucose 2′-sulfate and dehydrated 6′-C_{40}-hydroxyphthioceranoylglucose 2′-sulfate anions, respectively. These two ions consist of the glucose moiety originally bearing the lone acyl group and the sulfate substituent and were formed by further elimination of $C_6H_4O_2$ and $C_6H_6O_3$ fragments from the ion at m/z 957, respectively, supporting the possibility that a C_{40}-hydroxyphthioceranoyl is located at position 6′. This latter fragmentation process is supported by the MS^4 spectrum of the

dx.doi.org/10.1021/bi2012178 | Biochemistry 2011, 50, 9135–9147

Scheme 1. Fragmentation Processes Proposed for 2,3,6,6′-Tetraacyl-α,α′-D-trehalose 2′-Sulfate (sulfolipid II)[a]

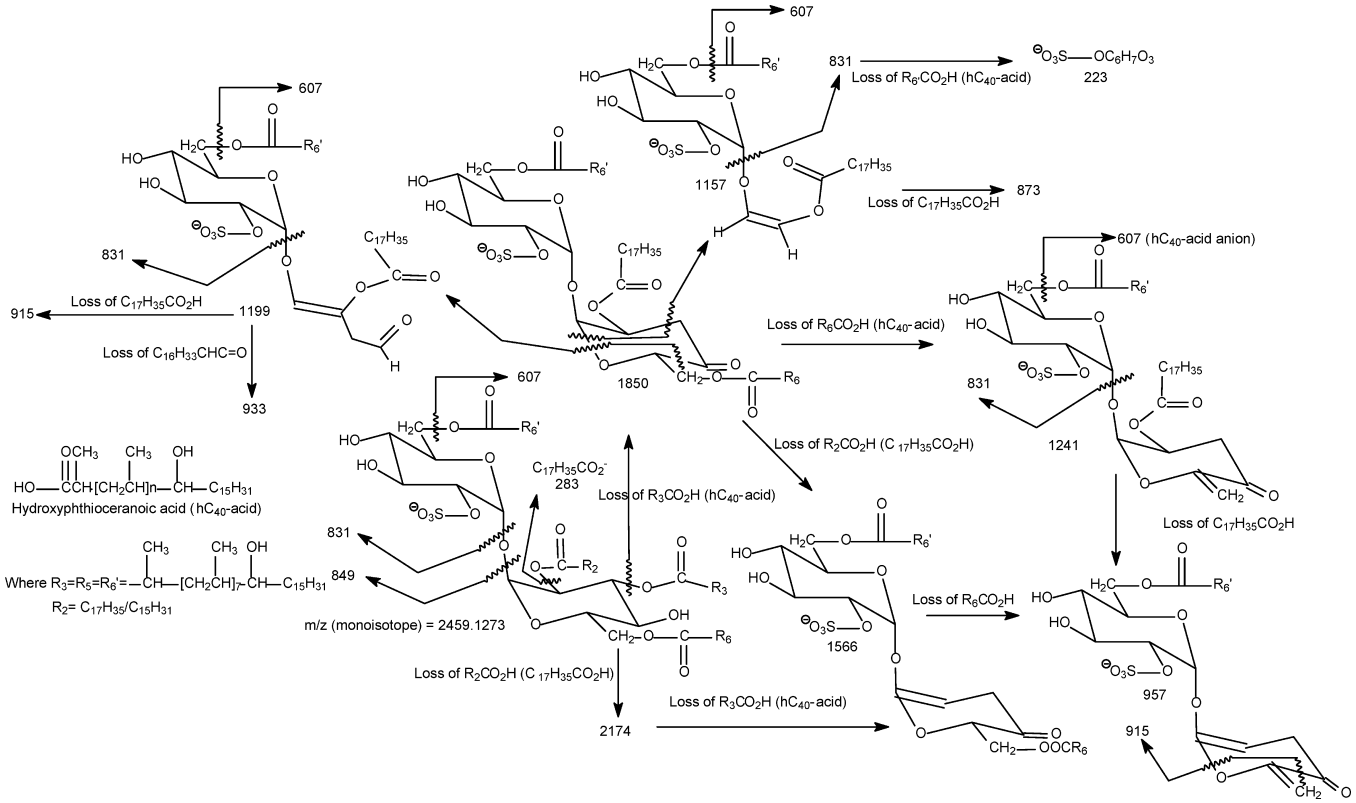

[a]Pathways for the most prominent $[M - H]^-$ ion at m/z 2459 (monoisotopic) mainly representing an [18:0,hC$_{40}$,hC$_{40}$,hC$_{40}$]-SL. The structures of the indicated fragment ions are supported by the elemental compositions deduced from accurate mass measurements via high-resolution MS^n mass spectrometry (see Table 1).

ion at m/z 957 [m/z 2459.1 → m/z 1566.3 → m/z 957.7 (Figure 3f)]. The MS^5 spectrum of the ion at m/z 831.5 [m/z 2459.1 → m/z 1566.3 → m/z 957.7 → m/z 831.5 (Figure 3g)] is dominated by the ion at m/z 607.5 (m/z 831.5 − m/z 224), representing a 6′-C$_{40}$-hydroxyphthioceranoic anion, and the ion at m/z 223, representing a dehydrated glucose 2′-sulfate anion (Scheme 1 and Figure 3b), confirming that the ion at m/z 831 indeed contains the glucose moiety originally bearing the lone acyl residue and the sulfate substituent and represents a 6′-C$_{40}$-hydroxyphthioceranoylglucose 2′-sulfate anion. These results indicate that the major ion at m/z 2459.1 represents a 2-stearoyl-3,6,6′-tris(2,4,6,8,10,12,14,16-octamethyl-17-hydroxydotriacontanoyl)-α,α′-D-trehalose 2′-sulfate ([18:0,hC$_{40}$,hC$_{40}$,hC$_{40}$]-SL). The fragmentation processes were further supported by the elemental compositions of the fragment ions obtained from the high-resolution CID and HCD tandem mass spectra (Table 1). The HCD MS^2 spectrum of the ion at m/z 2459.1 (Figure 3b) contained the tandem quadrupole-like spectrum, which is dominated by the hydroxyphthioceranoic acid anion at m/z 607 (measured mass of m/z 607.6032, calculated mass of m/z 607.6034) with a $C_{40}H_{79}O_3^-$ elemental composition, consistent with the suggested structure of 2,4,6,8,10,12,14,16-octamethyl-17-hydroxydotriacontanoyl acid, along with the homologous ions at m/z 691, 649, 635, 565, and 523 (Table 1). The characterization of hydroxyphthioceranoic acid, described below, was further achieved via its MS^n spectra.

In Figure 3c, the ion at m/z 1594.3 arising from further loss of 16:0-fatty acid residue is also present, consistent with the observation of the ion at m/z 2202.8 in Figure 3a. The results indicate the presence of the isomer bearing a 16:0-fatty acid substituent at position 2 and a C$_{40}$-hydroxyphthioceranoic acid residue most likely at position 3. The ion at m/z 1594.3 can also arise from losses that occur in a reversed manner (i.e., first loss of the palmitoyl group followed by a C$_{40}$-hydroxyphthioceranoic acid residue), similar to the formation of the ion at m/z 1568 described above. Further dissociation of the ion at m/z 1594.3 [m/z 2459.1 → m/z 1594.3 (Figure 3h)] yielded ions at m/z 985 and 957, arising from losses of C$_{38}$-hydroxyphthioceranoic and C$_{40}$-hydroxyphthioceranoic acids, respectively, along with ions at m/z 635 and 607, representing C$_{42}$-hydroxyphthioceranoic and C$_{40}$-hydroxyphthioceranoic anions, respectively. The results indicate the presence of C$_{42}$-hydroxyphthioceranoic and C$_{40}$-hydroxyphthioceranoic residues at positions 6 and 6′, respectively. The spectrum also contained the ions at m/z 859 and 831, corresponding to 6′-C$_{42}$-hydroxyphthioceranoylglucose 2′-sulfate and 6′-C$_{40}$-hydroxyphthioceranoylglucose 2′-sulfate anions, respectively. These results indicate that both the C$_{42}$- and C$_{40}$-hydroxyphthioceranoyl groups can reside at position 6′, suggesting the presence of 2-palmitoyl-3,6-bis(2,4,6,8,10,12,14,16-octamethyl-17-hydroxydotriacontanoyl)-6′-2,4,6,8,10,12,14,16-octamethyl-17-hydroxytetratriacontanoyl-α,α′-D-trehalose 2′-sulfate ([16:0,hC$_{40}$,hC$_{40}$,hC$_{42}$]-SL) and 2-palmitoyl-3,6′-bis(2,4,6,8,10,12,14,16-octamethyl-17-hydroxytetratriacontanoyl)-6-2,4,6,8,10,12,14,16-octamethyl-17-hydroxytetratriacontanoyl-α,α′-D-trehalose 2′-sulfate ([16:0,hC$_{40}$,hC$_{42}$,hC$_{40}$]-SL) isomers. The observation of these latter two isomers indicates that the 2-substituent appears to be restricted as previously reported,[2−4] while the substituents at positions 6 and 6′ are interchangeable.

dx.doi.org/10.1021/bi2012178|Biochemistry 2011, 50, 9135−9147

Table 1. Elemental Compositions of the Fragment Ions Obtained via High-Resolution CID and HCD MS^2 of the $[M - H]^-$ Ion of Sulfolipid at *m/z* 2459

nominal mass (*m/z*)	measured mass (Da)	calculated mass (Da)	elementary composition	nominal mass (*m/z*)	measured mass (Da)	calculated mass (Da)	elementary composition
2459	2459.1274	2456.1273	$C_{150}H_{289}O_{21}S$	1041	1041.7274	1041.7281	$C_{58}H_{105}O_{13}S$
2202	2202.8860	2202.8870	$C_{134}H_{257}O_{19}S$	999	999.6804	999.6812	$C_{55}H_{99}O_{13}S$
2174	2174.8547	2174.8557	$C_{132}H_{253}O_{19}S$	985	985.6645	985.6655	$C_{54}H_{97}O_{13}S$
1934	1934.6082	1934.6104	$C_{116}H_{221}O_{18}S$	957	957.6334	957.6342	$C_{52}H_{93}O_{13}S$
1892	1892.5634	1892.5635	$C_{113}H_{215}O_{18}S$	933	933.7065	933.7070	$C_{52}H_{10}1O_{11}S$
1864	1864.5292	1864.5322	$C_{111}H_{211}O_{18}S$	917	917.6386	917.6393	$C_{50}H_{93}O_{12}S$
1850	1850.5147	1850.5165	$C_{110}H_{209}O_{18}S$	901	901.6438	901.6444	$C_{50}H_{93}O_{11}S$
1836	1836.5026	1836.5009	$C_{109}H_{207}O_{18}S$	891	891.6583	891.6601	$C_{49}H_{95}O_{11}S$
1822	1822.4854	1822.4852	$C_{108}H_{205}O_{18}S$	877	877.6436	873.6444	$C_{48}H_{93}O_{11}S$
1808	1808.4676	1808.4695	$C_{107}H_{203}O_{18}S$	873	873.6490	873.6495	$C_{49}H_{93}O_{10}S$
1766	1766.4212	1766.4226	$C_{104}H_{197}O_{18}S$	859	859.6331	859.6338	$C_{48}H_{91}O_{10}S$
1692	1692.3864	1692.3858	$C_{101}H_{191}O_{16}S$	849	849.6127	849.6131	$C_{46}H_{89}O_{11}S$
1678	1678.3723	1678.3702	$C_{100}H_{189}O_{16}S$	847	847.5968	847.5975	$C_{46}H_{87}O_{11}S$
1650	1650.3378	1650.3389	$C_{98}H_{185}O_{16}S$	831	831.6021	831.6025	$C_{46}H_{87}O_{10}S$
1608	1608.2910	1608.2919	$C_{95}H_{179}O_{16}S$	747	747.5088	747.5086	$C_{40}H_{75}O_{10}S$
1594	1594.2756	1594.2763	$C_{94}H_{177}O_{16}S$	691	691.6970	691.6974	$C_{46}H_{91}O_3$
1566	1566.2441	1566.2450	$C_{92}H_{173}O_{16}S$	649	649.6502	649.6504	$C_{43}H_{85}O_3$
1538	1538.2130	1538.2137	$C_{90}H_{169}O_{16}S$	635	635.6345	645.6348	$C_{42}H_{83}O_3$
1524	1524.1961	1524.1980	$C_{89}H_{167}O_{16}S$	607	607.6032	607.6034	$C_{40}H_{79}O_3$
1510	1510.1821	1510.1824	$C_{88}H_{165}O_{16}S$	565	565.5564	565.5565	$C_{37}H_{73}O_3$
1482	1482.1506	1482.1511	$C_{86}H_{161}O_{16}S$	523	523.5092	523.5095	$C_{34}H_{67}O_3$
1241	1241.9047	1241.9058	$C_{70}H_{129}O_{15}S$	283	283.2643	283.2643	$C_{18}H_{35}O_2$
1213	1213.8732	1213.8745	$C_{68}H_{125}O_{15}S$	255	255.2333	255.2330	$C_{16}H_{31}O_2$
1199	1199.8941	1199.8952	$C_{68}H_{127}O_{14}S$	223	222.9921	222.9918	$C_6H_7O_7S$
1171	1171.8630	1171.8639	$C_{66}H_{123}O_{14}S$	204	204.9820	204.9812	$C_6H_5O_6S$
1157	1157.8445	1157.8453	$C_{65}H_{121}O_{14}S$				

Again, the structural assignments of the fragment ions are consistent with the elemental composition deduced from high-resolution mass measurements (Table 1). Collectively, the ion at *m/z* 2459.1 represents a major [18:0,hC_{40},hC_{40},hC_{40}]-SL isomer together with two minor isomers, [16:0,hC_{40},hC_{40},hC_{42}]-SL and [16:0,hC_{40},hC_{42},hC_{40}]-SL.

In Figure 3b, minor C_{46}-, C_{37}-, and C_{34}-hydroxyphthioceranoic anions at *m/z* 691, 565, and 523, respectively, were also observed, and the minor homologous ions at *m/z* 1766, 1892, and 1934 arising from losses of the C_{46}-, C_{37}-, and C_{34}-hydroxyphthioceranoic acids, respectively, were also present in Figure 3a. These results indicate the presence of the minor isomers possessing the C_{46}-, C_{37}-, and C_{34}-hydroxyphthioceranoic acid substituents. Further dissociation of the ion at *m/z* 1524 [*m/z* 2459.1 → *m/z* 1524.2 (data not shown)] yielded the ion pairs at *m/z* 957/915 and 999/873 arising from losses of C_{37}/C_{40}- and C_{34}/C_{43}-hydroxyphthioceranoic acids, together with the C_{37}-, C_{40}-, C_{34}-, and C_{43}-hydroxyphthioceranoic anions at *m/z* 565, 607, 523, and 649, respectively. The results support the presence of [18:0,hC_{46},hC_{40},hC_{37}]-SL and [18:0,hC_{46},hC_{43},hC_{34}]-SL isomers. The presence of these minor isomers is consistent with the observation of the minor ion at *m/z* 1524 in Figure 3d, arising from consecutive losses of 18:0-fatty acid and C_{46}-hydroxyphthioceranoic acid. The structural assignments were also supported by accurate mass measurements (Table 1).

Similarly, the MS^2 spectrum of the ion at *m/z* 2543.2 (Figure 4a) contained the ions at *m/z* 2286 and 2258, arising from loss of 16:0- and 18:0-fatty acid residues, respectively. The ions at *m/z* 1934, 1906, 1892, and 1850 arise from losses of C_{40}-, C_{42}-, C_{43}-, and C_{46}-hydroxyphthioceranoic residues, respectively, at position 3. The sequential losses of the 18:0-fatty acid at position 2 gave rise to ions at *m/z* 1650, 1622, 1608, and 1566, respectively, while the ion at *m/z* 1678 mainly arise from further loss of a 16:0-fatty acid residue from the ion at *m/z* 1934. The profile of the ion set of *m/z* 1934, 1906, 1892, and 1850 is similar to that of the ion set of *m/z* 1650, 1622, 1608, and 1566 (Figure 4a), consistent with the fragmentation mechanisms that first eliminate the 3-hydroxyphthioceranoic acid residue followed by loss of the 18:0-fatty acid at position 2 (or vice verse) as described above. The results indicate that the ion at *m/z* 2543 consists of the isomers in which positions 2 and 3 have hC_{40}/18:0-, hC_{42}/18:0-, hC_{43}/18:0-, and hC_{46}/18:0- and hC_{40}/16:0-fatty acid substituents. The prominence of the these ion pairs (e.g., ions at *m/z* 1934 and 1650), again, indicates the preferential losses of the substituents at positions 2 and 3 over those located at position 6 or 6′, which have the greater stability toward acid or alkaline hydrolysis as compared with the substituents at positions 2 and 3.[5]

Further dissociation of the ion at *m/z* 1650 [*m/z* 2543 → *m/z* 1650 (Figure 4b)] yielded the major ions at *m/z* 1041 and 999, together with the ion at *m/z* 957, arising from losses of C_{40}-, C_{43}-, and C_{46}-hydroxyphthioceranoic acids, respectively. The results are consistent with the observation of the major C_{40}- and C_{46}-hydroxyphthioceranoic acid anions at *m/z* 607 and 691, respectively, as well as the presence of the C_{43}-hydroxyphthioceranoic acid anion at *m/z* 649. The spectrum also contained the 6′-C_{40}-, 6′-C_{43}-, and 6′-C_{46}-hydroxyphthioceranoyl glucose-2′-sulfate anions at *m/z* 831, 873, and 915, respectively, indicating that the ion at *m/z* 2543 consists of major [18:0,hC_{40},hC_{40},hC_{46}]-SL and [18:0,hC_{40},hC_{46},hC_{40}]-SL

dx.doi.org/10.1021/bi2012178 | *Biochemistry* 2011, 50, 9135–9147

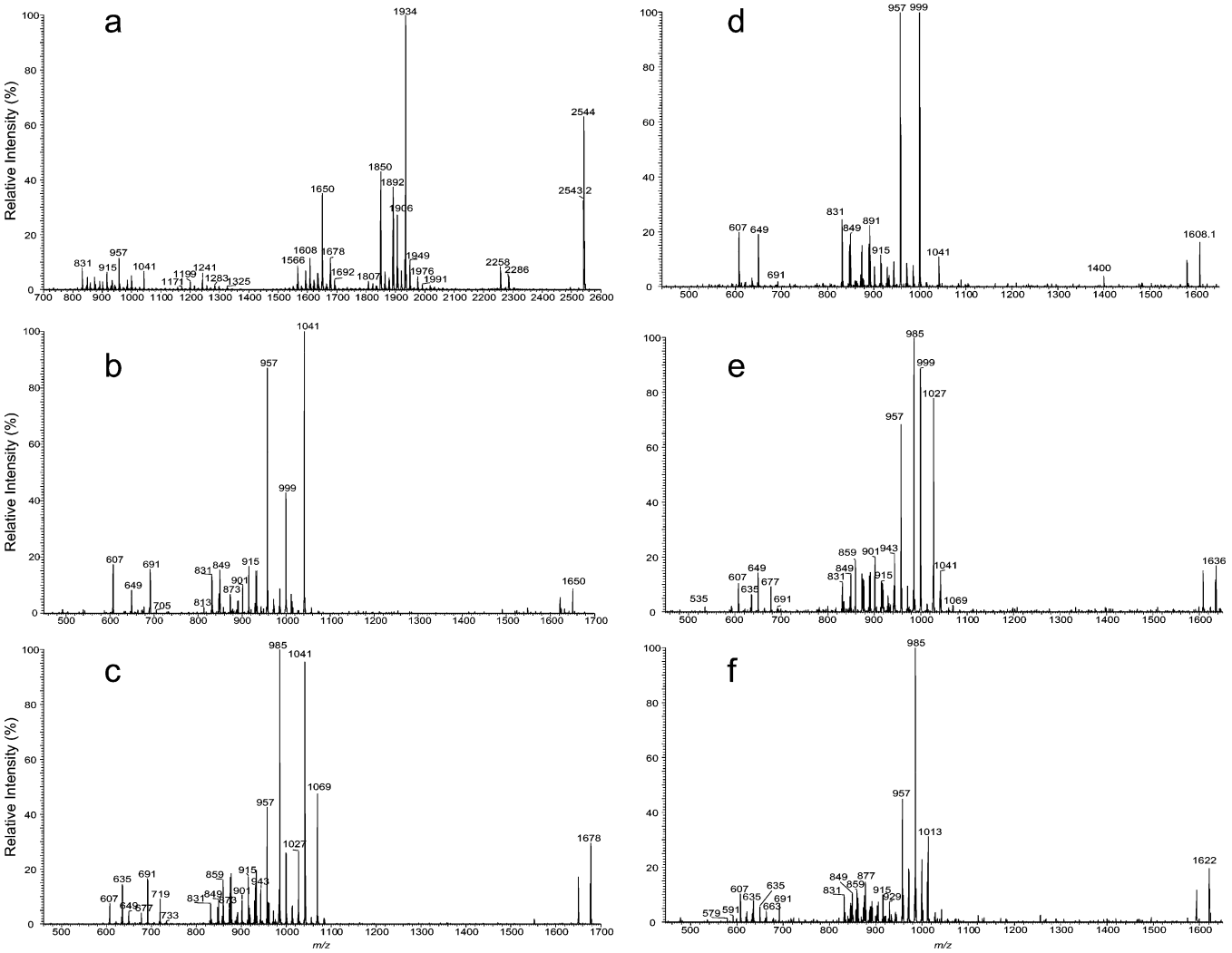

Figure 4. LIT CID MS^2 spectrum of the ion at m/z 2543 (a) and sequential MS^3 spectra of the ions at m/z 1650 (m/z 2543 → m/z 1650) (b), m/z 1678 (m/z 2543 → m/z 1678) (c), m/z 1608 (m/z 2543 → m/z 1608) (d), m/z 1636 (m/z 2543 → m/z 1636) (e), and m/z 1622 (m/z 2543 → m/z 1622) (f).

isomers together with a minor [18:0,hC_{40},hC_{43},hC_{43}]-SL isomer.

MS^3 spectra of the ion at m/z 1678 [m/z 2543 → m/z 1678 (Figure 4c)] yielded ions at m/z 1041 (loss of m/z 636), m/z 985 (loss of m/z 692), m/z 1069 (loss of m/z 608), m/z 957 (loss of m/z 720), m/z 999 (loss of m/z 678), and m/z 1027 (loss of m/z 650), consistent with the observation of the hydroxyphthioceranoic anions at m/z 635, 691, 607, 719, 677, and 649 that represent C_{42}-, C_{46}-, C_{40}-, C_{48}-, C_{45}-, and C_{43}-hydroxyphthioceranoic acid, respectively. The spectrum also contained ions at m/z 859, 915, 831, 943, 901, and 873, indicating the presence of 6′-C_{42}-, 6′-C_{46}-, 6′-C_{40}-, 6′-C_{48}-, 6′-C_{45}-, and 6′-C_{43}-hydroxyphthioceranoylglucose 2′-sulfate anions, respectively, as seen earlier. The observation of the abundant ion pairs at m/z 1041 (loss of hC_{42}) and m/z 985 (loss of hC_{46}) signifies the presence of the major [16:0,hC_{40},hC_{42},hC_{46}]-SL and [16:0,hC_{40},hC_{46},hC_{42}]-SL isomers, while the m/z 1069/957 pairs led to the assignment of the [16:0,hC_{40},hC_{40},hC_{48}]-SL and [16:0,hC_{40},hC_{48},hC_{40}]-SL isomers; the minor m/z 999/1027 ion pairs led to the assignment of the [16:0,hC_{40},hC_{43},hC_{45}]-SL and [16:0,hC_{40},hC_{45},hC_{43}]-SL isomers.

As described above, the ions at m/z 1566 and 1594 arose from the consecutive losses of C_{46}- and C_{44}-hydroxyphthioceranoic acids, respectively, followed by loss of the 18:0-fatty acid residue at C-2. Further dissociation of the ion at m/z 1566 (m/z 2543 → m/z 1566) yielded a spectrum identical to that shown in Figure 4c, indicating the presence of C_{40}-hydroxyphthioceranoic acid residues at positions 6 and 6′. The results led to the assignment of the [18:0,hC_{46},hC_{40},hC_{40}]-SL isomer, which is a positional isomer to [18:0,hC_{40},hC_{40},hC_{46}]-SL and [18:0,hC_{40},hC_{46},hC_{40}]-SL as seen earlier. The profile of the MS^3 spectrum of the ion at m/z 1594 [m/z 2543 → m/z 1594 (not shown)] is also similar to that shown in Figure 4f and is dominated by the ions at m/z 985 (m/z 1594 − m/z 608) and m/z 957 (m/z 1594 − m/z 636), indicating the presence of [18:0,hC_{44},hC_{40},hC_{42}]-SL. Similarly, the MS^3 spectrum of the ion at m/z 1608 [m/z 2543 → m/z 1608 (Figure 4d)] is dominated by the ions at m/z 999 and 957, arising from losses of the C_{40}- and C_{43}-hydroxyphthioceranoic acids, respectively, consistent with the observation of the C_{40}- and C_{43}-hydroxyphthioceranoic anions at m/z 607 and 649, respectively. These results further support the presence of the [18:0,hC_{40},hC_{43},hC_{43}]-SL isomer.

dx.doi.org/10.1021/bi2012178 | *Biochemistry* 2011, 50, 9135–9147

Table 2. High-Resolution ESI Mass Spectrum of the $[M - H]^-$ Ions of Hydroxyphthioceranoic (★) and Phthioceranoic (#) Acids Generated by Skimmer CID of the SLs

measured mass (Da)	calculated mass (Da)	elemental composition	relative intensity (%)	structure (class)
383.3528	383.3531	$C_{24}H_{47}O_3$	1.33	★
397.3685	397.3687	$C_{25}H_{49}O_3$	0.66	★
409.4048	409.4051	$C_{27}H_{53}O_2$	1.88	#
411.3844	411.3844	$C_{26}H_{51}O_3$	0.20	★
423.4205	423.4208	$C_{28}H_{55}O_2$	3.08	#
425.3997	425.4000	$C_{27}H_{53}O_3$	1.59	★
437.4362	437.4364	$C_{29}H_{57}O_2$	4.29	#
439.4154	439.4157	$C_{28}H_{55}O_3$	0.12	★
451.4517	451.4521	$C_{30}H_{59}O_2$	2.74	#
453.4311	453.4513	$C_{29}H_{57}O_3$	0.02	★
465.4674	465.4677	$C_{31}H_{61}O_2$	0.83	#
467.4467	467.4470	$C_{30}H_{59}O_3$	0.22	★
479.4831	479.4834	$C_{32}H_{63}O_2$	4.68	#
481.4623	481.4626	$C_{31}H_{61}O_3$	1.95	★
493.4987	493.4990	$C_{33}H_{65}O_2$	1.91	#
495.4780	495.4783	$C_{32}H_{63}O_3$	0.69	★
507.5145	507.5147	$C_{34}H_{67}O_2$	2.87	#
509.4938	509.4939	$C_{33}H_{65}O_3$	4.19	★
521.5301	521.5303	$C_{35}H_{69}O_2$	0.74	#
523.5094	523.5096	$C_{34}H_{67}O_3$	9.64	★
535.5458	535.5460	$C_{36}H_{71}O_2$	1.25	#
537.5250	537.5252	$C_{35}H_{69}O_3$	1.04	★
549.5613	549.5616	$C_{37}H_{73}O_2$	2.04	#
551.5407	551.5409	$C_{36}H_{71}O_3$	2.22	★
563.5767	563.5773	$C_{38}H_{75}O_2$	0.25	#
565.5562	565.5565	$C_{37}H_{73}O_3$	9.00	★
577.5926	577.5929	$C_{39}H_{77}O_2$	0.82	#
579.5719	579.5722	$C_{38}H_{75}O_3$	0.64	★
591.6082	591.6086	$C_{40}H_{79}O_2$	4.69	#
593.5875	593.5878	$C_{39}H_{77}O_3$	3.32	★
605.6239	605.6242	$C_{41}H_{81}O_2$	0.86	#
607.6031	607.6034	$C_{40}H_{79}O_3$	100.00	★
619.6394	619.6399	$C_{42}H_{83}O_2$	2.64	#
621.6187	621.6191	$C_{41}H_{81}O_3$	13.72	★
633.6551	633.6555	$C_{43}H_{85}O_2$	2.65	#
635.6343	635.6348	$C_{42}H_{83}O_3$	40.78	★
647.6707	647.6712	$C_{44}H_{87}O_2$	1.18	#
649.6499	649.6504	$C_{43}H_{85}O_3$	36.36	★
661.6863	661.6868	$C_{45}H_{89}O_2$	2.53	#
663.6655	663.6661	$C_{44}H_{87}O_3$	6.07	★
675.7019	675.7026	$C_{46}H_{91}O_2$	1.01	#
677.6811	677.6817	$C_{45}H_{89}O_3$	12.44	★
689.7172	689.7181	$C_{47}H_{93}O_2$	0.22	#
691.6968	691.6974	$C_{46}H_{91}O_3$	44.16	★
703.7331	703.7338	$C_{48}H_{95}O_2$	0.48	#
705.7124	705.7130	$C_{47}H_{93}O_3$	5.18	★
719.7280	719.7287	$C_{48}H_{95}O_3$	8.40	★
731.7641	731.7651	$C_{50}H_{99}O_2$	0.01	#
733.7437	733.7443	$C_{49}H_{97}O_3$	11.24	★
745.7802	745.7807	$C_{51}H_{101}O_2$	0.03	#
747.7592	747.7600	$C_{50}H_{99}O_3$	1.23	★
759.7960	759.7964	$C_{52}H_{103}O_2$	0.03	#
761.7749	761.7756	$C_{51}H_{101}O_3$	0.60	★
775.7905	775.7913	$C_{52}H_{103}O_3$	0.68	★

More minor isomeric structures were revealed by MS^3 of the ions at m/z 1636 [m/z 2543 → m/z 1636 (Figure 4e)] and m/z 1622 [m/z 2543 → m/z 1622 (Figure 4f)]. The former spectrum contained the m/z 985/999 ion pair from loss of C_{43}-/C_{42}-hydroxyphthioceranoic acids, as well as the m/z 1027/957 ion pair from loss of the C_{40}-/C_{44}-hydroxyphthioceranoic acids. These results led to the assignment of the [18:0,hC_{41},hC_{43},hC_{42}]-SL and [18:0,hC_{41},hC_{40},hC_{45}]-SL isomers. The latter spectrum (Figure 4f) is dominated by ion pairs at m/z 985/985 and 957/1013, arising from losses of C_{42}-/C_{42}-hydroxyphthioceranoic acids and C_{43}-/C_{41}-hydroxyphthioceranoic acids, respectively, leading to assignment of the [18:0,hC_{42},hC_{42},hC_{42}]-SL and [18:0,hC_{42},hC_{43},hC_{41}]-SL isomers. Collectively, the ion at m/z 2543 consists of more than 12 isomers in which [18:0,hC_{40},hC_{40},hC_{46}]-SL and [18:0,hC_{40},hC_{43},hC_{43}]-SL predominate. This structural complexity in a single species of SLs was recently reported with less detail by Layre et al.[21]

To reveal the shortest hydroxyphthioceranoic chain that constitutes the SL-II molecules, MS^n was conducted on the low-mass end ion at m/z 2122.8. The MS^2 spectrum (see Figure S2a of the Supporting Information) is dominated by the ion at m/z 1640, arising from loss of C_{31}-hydroxyphthioceranoic acid, together with an ion at m/z 1356 from the further loss of 18:0-fatty acid, indicating the presence of 18:0- and hC_{31}-acids at positions 2 and 3, respectively. Further dissociation of the ion at m/z 1356 [m/z 2122.8 → m/z 1356 (Figure S2b of the Supporting Information)] gave rise to ion pairs at m/z 957/747 and 873/831 by further elimination of C_{25}-/C_{40}-hydroxyphthioceranoic and C_{31}-/C_{34}-hydroxyphthioceranoic acids, respectively. These results led to the assignment of the [18:0,hC_{31},hC_{25},hC_{40}]-SL and [18:0,hC_{31},hC_{31},hC_{34}]-SL structures. The loss of the hC_{25}/hC_{40}-acids is consistent with the observation of the hC_{25}/hC_{40} anion at m/z 397 and 607 (Figure S2b of the Supporting Information). The ion at m/z 397 corresponds to a 2,4,6-trimethyl-7-hydroxydodecanoic acid anion possessing two repeating isopropyl [$CH_2CH(CH_3)$] units. This short chain hydroxyphthioceranoic acid chain was recently reported by Layre et al.[21] but not previously by Goren.[4] The structural assignment is consistent with the observation of the ion pairs at m/z 1724/1514 and 1640/1598 in Figure S2a of the Supporting Information, arising from losses of hC_{25}/hC_{40} (m/z 398/608) and hC_{31}/hC_{34} (m/z 482/524). The observation of the ion at m/z 1384 from the consecutive losses of C_{31}-hydroxyphthioceranoic acid and 16:0-fatty acid (Figure S2b of the Supporting Information), together with the ion pairs at m/z 859/873, 775/957, and 747/985 [m/z 2122.8 → m/z 1384 (Figure S2c of the Supporting Information)] arising from loss of hC_{34}/hC_{33}, hC_{40}/hC_{27}, and hC_{42}/hC_{25}, respectively, readily gives assignments of the [16:0,hC_{31},hC_{33},hC_{34}]-SL, [16:0,hC_{31},hC_{27},hC_{40}]-SL, and [16:0,hC_{31},hC_{25},hC_{42}]-SL isomers.

For further insight into the long hydroxyphthioceranoic chain that constitutes SL-II, the high-mass end ion at m/z 2795.5 was subjected to CID. Again, the MS^2 spectrum of the ion at m/z 2795.5 (Figure S3a of the Supporting Information) contained homologous ions at m/z 2102.8 and 2060.7, arising from losses of C_{46}- and C_{49}-hydroxyphthioceranoic acids, respectively, together with the ions at m/z 1776 and 1818 arising from further loss of 18:0-fatty acid. MS^3 of the ion at m/z 1776 [m/z 2795.5 → m/z 1776 (Figure S3b of the Supporting Information)] gave rise to the ion pair at m/z 1041/1083 by loss of C_{49}-/C_{46}-hydroxyphthioceranoic acid, consistent with the observation of the C_{49}- and C_{46}-hydroxyphthioceranoic acid anions at m/z 733 and 691,

dx.doi.org/10.1021/bi2012178 | Biochemistry 2011, 50, 9135–9147

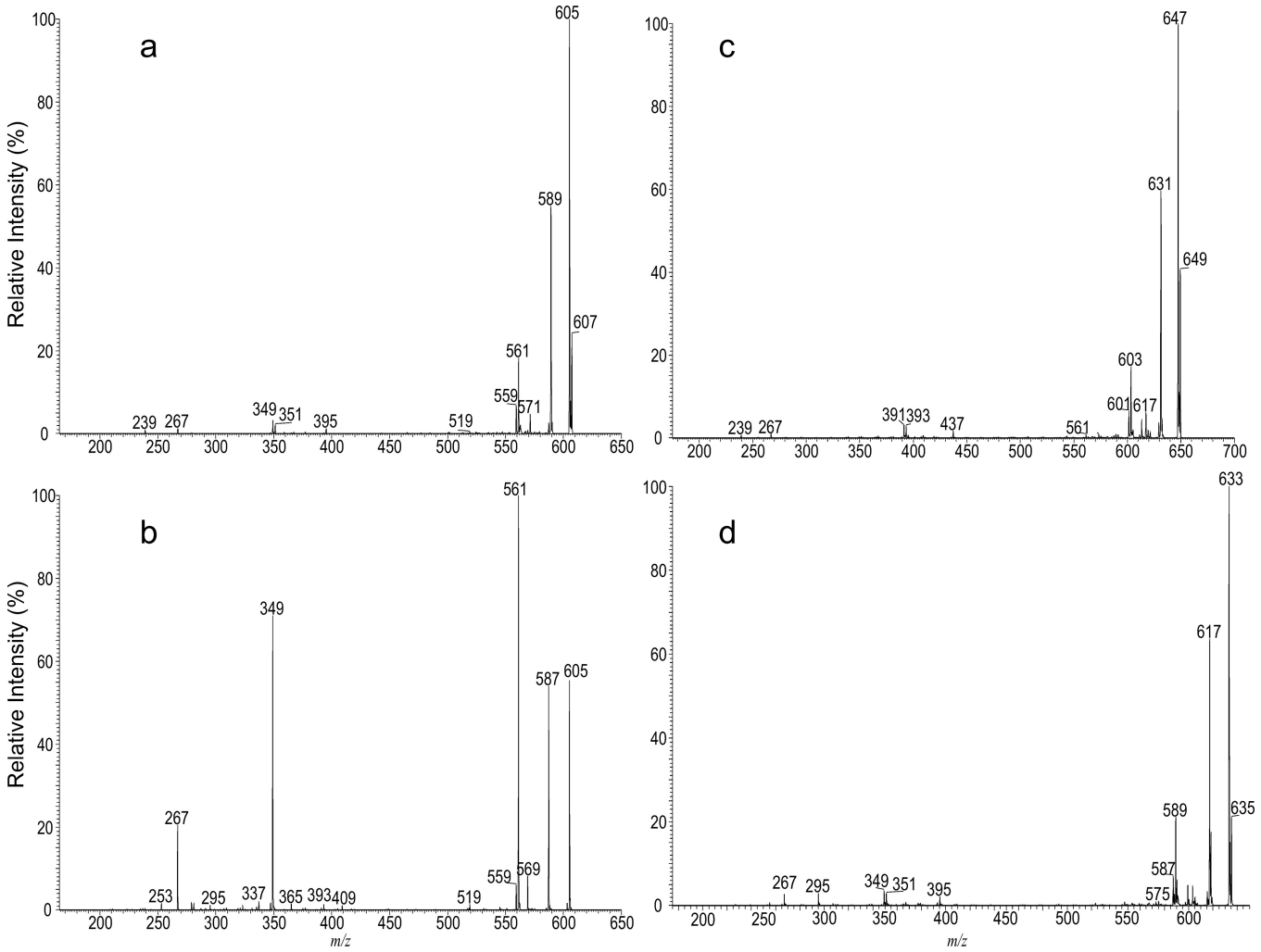

Figure 5. CID MS^2 spectrum of the $[M - H]^-$ ion of C_{40}-hydroxyphthioceranoic acid at m/z 607 generated by skimmer CID (a), its MS^3 spectrum at m/z 605 (m/z 607 → m/z 605) (b), and the MS^3 spectra of the C_{43}-hydroxyphthioceranoic ion at m/z 649 (m/z 2459 → m/z 649) (c) and the C_{42}-hydroxyphthioceranoic ion at m/z 635 (m/z 2543 → m/z 635) (d).

respectively. The spectrum also contained the 6′-C_{49}- and 6′-C_{46}-hydroxyphthioceranoylglucose 2′-sulfate anions at m/z 957 and 915, respectively, indicating that the ion represents the major [18:0,hC$_{49}$,hC$_{49}$,hC$_{46}$]-SL and [18:0,hC$_{49}$,hC$_{46}$,hC$_{49}$]-SL isomers. The MS^3 spectrum of the ion at m/z 1818 [m/z 2795.5 → m/z 1818 (Figure S3c of the Supporting Information)] is dominated by the ion pair at m/z 1083/1083 arising from elimination of 6-C_{49}/6′-C_{49}-hydroxyphthioceranoic acid, indicating the presence of the [18:0,hC$_{46}$,hC$_{49}$,hC$_{49}$]-SL isomer. The spectrum (Figure S3c of the Supporting Information) also contained the ion pair at m/z 1125/1041 arising from further losses of C_{46}/C_{52}-hydroxyphthioceranoic acid, indicating the presence of the minor [18:0,hC$_{46}$,hC$_{46}$,hC$_{52}$]-SL isomer. The presence of this minor isomer is consistent with the observation of the ion at m/z 775 and 691 (Figure S3c of the Supporting Information). The ion at m/z 775 represents a 2,4,6,8,10,12,14,16,18,20,22,24-dodecamethyl-22-hydroxytetracontanoic anion possessing 11 isopropyl repeat units, which is one isopropyl unit longer than that previously reported by Goren.[4]

Characterization of the Multiple-Methyl-Branched Hydroxyphthioceranoic Acid. Upon being subjected to ESI with skimmer CID (100 V), the SL extract yielded a whole array of anions in the mass range from m/z 383 to 775, corresponding to the $[M - H]^-$ ions of hydroxyphthioceranoic and phthioceranoic acids (Table 2). Elemental compositions deduced from high-resolution mass measurements confirmed the presence of the major hydroxyphthioceranoic acid ion series at m/z 383, 397, ..., 607, ..., and 775, together with the minor phthioceranoic acid ion series at m/z 409, 423, ..., 591, ..., and 703 (Table 2). The summed percentage of the ion abundance ($\sum$%) of the hydroxyphthioceranoic acid ion series is 88%, and that of the phthioceranoic acid ion series is 12%. These data gave a molar ratio of SL-II to SL-I of ~2/1, based on the fact that SL-II consists of three hydroxyphthioceranoic acid residues and SL-I consists of two hydroxyphthioceranoic acid and one phthioceranoic acid residues, and both the hydroxyphthioceranoic and phthioceranoic acid residues were cleaved by skimmer CID in the same manner. These results further support the notion that the principal sulfolipid from H37Rv is SL-II, and SL-I is the minor component (Figure 2 and Table S1 of the Supporting Information). The ion at m/z 607 is predominant [100% (Table 2)], consistent with the earlier report that the major hydroxyphthioceranoic acid in SLs is a 2,4,6,8,10,12,14,16-octamethyl-17-hydroxydotriacontanoic acid.[4] The characterization of the structure of hydroxydo-

dx.doi.org/10.1021/bi2012178 | Biochemistry 2011, 50, 9135–9147

Scheme 2. Fragment Ions Observed in the MS^n Spectra of the Major Hydroxyphthioceranoic Acid Substituents in SL-II and the Proposed Fragmentation Pathways Leading to Ion Formation and Structure Identification[a]

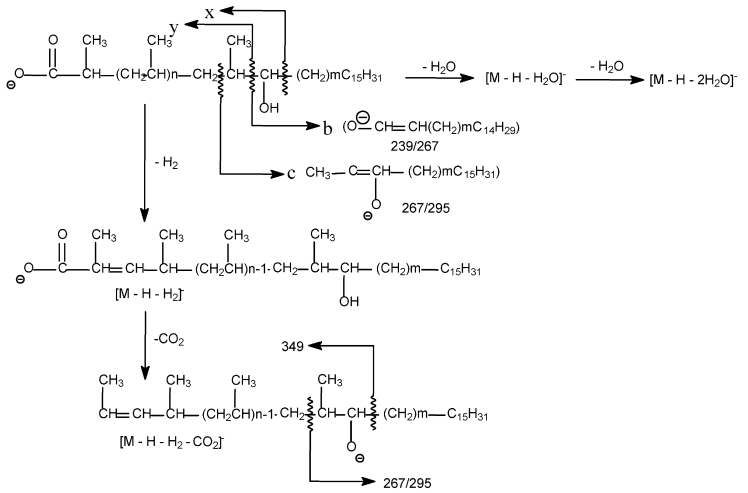

m	n	[M - H]$^-$	[M-H-H_2]$^-$	[M-H-H_2O]$^-$	[M-H-$2H_2O$]$^-$	[M-H-H_2-CO_2]$^-$	x	y	b	c	x-CO_2	x-H_2-CO_2
0	7	607	605	589	571	561	395	367	239	267	351	349
0	8	649	647	631	613	603	437	409	239	267	393	391
0	9	691	689	673	655	645	479	451	239	267	435	433
0	10	733	731	715	697	687	493	465	239	267	477	475
2	7	635	633	617	599	589	395	367	267	295	351	349

[a]The structures of the indicated fragment ions are supported by high-resolution LIT MS^n experiments (data not shown).

triacontanoic acids using MS^n and high-resolution mass spectrometry is described below.

The MS^2 spectrum of the ion at m/z 607 generated by skimmer CID on the sulfolipid mixture (Figure 5a) is identical to the MS^3 spectrum of the ion at m/z 607 [m/z 2459 → m/z 607 (not shown)] arising from dissociation of the ion at m/z 2459 (in this acquisition, the Q value of the ion trap for the MS^2 experiment was set to 0.2 to trap the ion at m/z 607 for further dissociation using MS^3). The spectrum (Figure 5a) contained the ion at m/z 395, arising from elimination of the $C_{15}H_{32}$ residue by cleavage of the C−C bond next to the hydroxyl group distal to the carboxylate terminal, together with the ion at m/z 367 by loss of a $C_{15}H_{31}CHO$ residue via cleavage of the C−C bond flanking the hydroxyl group in the vicinity of the carboxylate group. The cleavage of this latter bond is consistent with the observation of the ion at m/z 239, representing the deprotonated ion of $C_{15}H_{31}CHO$ (i.e., $C_{14}H_{29}CH{=}CHO^-$ ion) (Scheme 2). The spectrum also contained the ion at m/z 267, arising from cleavage of the C−C bond bearing the methyl branch most distal to the carboxylate terminal. This structural information suggests the presence of a hydroxyl group at C-17. The predominant ions at m/z 605 and 589 arose from losses of H_2 and H_2O, respectively; while the ion at m/z 561 arose from further loss of CO_2 from the ion at m/z 605 and gave rise to the ion at m/z 349 by further elimination of a $C_{15}H_{32}$ residue. This fragmentation process is further supported by the MS^4 spectrum of the ions at m/z 605 (Figure 5b) and m/z 561 (data not shown). The ion at m/z 351 (607 − $C_{15}H_{32}$ − CO_2) may arise from primary loss of a $C_{15}H_{32}$ residue followed by further losses of CO_2 (Scheme 2). The assignments of the fragment ions were further supported by the elemental compositions deduced from high-resolution mass measurements (data not shown). The results are consistent with structural assignment of 2,4,6,8,10,12,14,16-octamethyl-17-hydroxydotriacontanoic acid previously defined by Goren et al.[4]

The MS^2 spectrum of the ion at m/z 649 (also generated via skimmer CID) and the MS^3 spectrum of the ion at m/z 649 [m/z 2459 → m/z 649 (Figure 5c)] are identical and contained ions at m/z 437, 391, and 393, which are 42 Da (C_3H_6) heavier than the analogous ions at m/z 395, 349, and 351, respectively, seen in Figure 5a, indicating the presence of an additional isopropyl group along the fatty acyl chain. The spectrum also contained the ions at m/z 239 and 267, indicating the presence of the same $C_{15}H_{31}$ terminal group, together with the ions at m/z 647 (649 − H_2), 631 (649 − H_2O), and 603 (647 −CO_2) that are analogous to ions at m/z 605, 589, and 561, respectively, as seen in Figure 5a. The results indicate that the ion at m/z 649 represents a deprotonated 2,4,6,8,10,12,14,16,18-nonamethyl-19-hydroxytetratriacontanoic acid anion. Similar mass shifts of the analogous ions were also seen in the MS^3 spectra of the ion at m/z 691 (m/z 2543 → m/z 691) and m/z 733 (m/z 2795 → m/z 733) (Scheme 2), suggesting the presence of the structures of 2,4,6,8,10,12,14,16,18,20-decamethyl-21-hydroxyhexatriacontanoic acid and 2,4,6,8,10,12,14,16,18,20,22-undecamethyl-23-hydroxyoctatriacontanoic acid, respectively. The observation of the ion series of m/z 397, 439, 481, 523, 565, 607, 649, 691, 735, and 775 (Table 2) is in agreement with the suggested structures of $^-$OOC-CH(CH_3)-(CH_2CHCH_3)$_n$CH(OH)-$C_{15}H_{31}$ (n = 2−11) for hydroxyphthioceranoic acids. The C_{25}-hydroxyphthioceranoic acid at m/z 397 (n = 2) and the C_{52}-hydroxyphthioceranoic acid at m/z 775 (n = 11) are consistent with the observation of these two ions in the earlier structural assignment for the SL-II species at m/z 2122 (Figure S2 of the Supporting Information) and m/z 2795 (Figure S3 of the Supporting Information), respectively.

Again, MS^2 and MS^3 of the ion at m/z 635 [m/z 2543 → m/z 635 (Figure 5d)] yielded ions analogous to those seen in

dx.doi.org/10.1021/bi2012178|*Biochemistry* 2011, 50, 9135−9147

Figure 5a–c. The spectrum contained the ions at m/z 395, 351, and 349, identical to those seen in Figure 5a. However, the ions at m/z 267 and 295 are 28 Da heavier than the analogous ions at m/z 239 and 267, respectively (Scheme 2), seen in Figure 5a. The results indicate the presence of the structure of 2,4,6,8,10,12,14,16-octamethyl-17-hydroxyditriacontanoic acid, in which a terminal $C_{17}H_{35}$ rather than a $C_{15}H_{31}$ residue was attached to the same carbon that possesses the hydroxyl group. Homologous ions were seen at m/z 425, 467, 509, 551, 593, 635, 677, and 719, representing the ion series possessing the $^{-}OOC\text{-}CH(CH_3)(CH_2CHCH_3)_nCH(OH)C_{17}H_{35}$ structure, in which the homologous hydroxyphthioceranoic acids (n = 3–9) that differed by a repeat C_3 (isopropyl) unit are present, in agreement with the previous findings.[4]

CONCLUSIONS

Using high-resolution LIT MS^n, we made assignments for the complex structures of sulfolipids of *M. tuberculosis* H37Rv and confirmed that SL-II, not SL-I, predominates in the sulfolipid family, similar to the recent report by Layre et al. who used a different approach.[21] Thus, care should be taken when referring to the molecular structures of the major SL families as not to misassign the structures, if Goren's original designations of the SL families are to be followed. We verified that differences in culture media or extraction methods would not account for differences in the relative abundance of SL-I and SL-II. Under all culture conditions tested, SL-II is always more abundant than SL-I, and extraction with decylamine in hexane was more efficient for extracting the SL families. We also revealed the detailed structures of each of the SL-II species, with many isomers arising not only from the presence of the stearoyl or palmitoyl at position 2 but also from the various combinations of different chain lengths of the hydroxyphthioceranoic acid substituents located at positions 6 and 6′ of the trehalose backbone. Thus, hundreds of structures are present in the entire SL-II family. This immense structural diversity has not been reported previously and has been seen in other important lipid families such as mycolic acids, phosphatidylinositol mannosides, and trehalose dimycolates in our recent studies.[22−24]

ASSOCIATED CONTENT

Supporting Information

Additional observations and data. This material is available free of charge via the Internet at http://pubs.acs.org.

AUTHOR INFORMATION

Corresponding Author

*Box 8127, Washington University School of Medicine, 660 S. Euclid Ave., St. Louis, MO 63110. Telephone: (314) 362-0056. Fax: (314) 362-7641. E-mail: fhsu@im.wustl.edu.

Present Address

[§]Cornell nanoscale facility, Cornell University, Ithaca, NY 14853.

Funding

Supported by U.S. Public Health Service Grants P41-RR00954 (J.T.), P60-DK20579 (J.T.), and P30-DK56341 (J.T.).

ACKNOWLEDGMENTS

We thank Dr. Weidong Cui of the Department of Chemistry (Washington University, St. Louis, MO) for obtaining the FT-ICR mass spectrum. A SL standard was received as part of National Institute of Allergy and Infectious Disease Contract HHSN266200400091C, entitled "Tuberculosis Vaccine Testing and Research Materials", which was awarded to CSU.

ABBREVIATIONS

CID, collision-induced dissociation; ESI, electrospray ionization; MS, mass spectrometry; MS^n, multiple-stage tandem mass spectrometry; LIT, linear ion-trap; FT, Fourier transform.

REFERENCES

(1) Middlebrook, G., Coleman, C. M., and Schaefer, W. B. (1959) Sulfolipid from Virulent Tubercle bacilli. *Proc. Natl. Acad. Sci. U.S.A. 45*, 1801–1804.

(2) Goren, M. B. (1970) Sulfolipid I of *Mycobacterium tuberculosis*, strain H37Rv. I. Purification and properties. *Biochim. Biophys. Acta 210*, 116–126.

(3) Goren, M. B. (1970) Sulfolipid I of *Mycobacterium tuberculosis*, strain H37Rv. II. Structural studies. *Biochim. Biophys. Acta 210*, 127–138.

(4) Goren, M. B., Brokl, O., and Das, B. C. (1976) Sulfatides of *Mycobacterium tuberculosis*: The structure of the principal sulfatide (SL-I). *Biochemistry 15*, 2728–2735.

(5) Goren, M. B., Brokl, O., Das, B. C., and Lederer, E. (1971) Sulfolipid I of *Mycobacterium tuberculosis*. Strain H37RV. Nature of the Acyl Substituents. *Biochemistry 10*, 72–81.

(6) Okamoto, Y., Fujita, Y., Naka, T., Hirai, M., Tomiyasu, I., and Yano, I. (2006) Mycobacterial sulfolipid shows a virulence by inhibiting cord factor induced granuloma formation and TNF-α release. *Microb. Pathog. 40*, 245–253.

(7) Kato, M., and Goren, M. B. (1974) Synergistic action of cord factor and mycobacterial sulfatides on mitochondria. *Infect. Immun. 10*, 733–741.

(8) Goren, M. B., D'Arcy Hart, P., Young, M. R., and Armstrong, J. A. (1976) Prevention of phagosome-lysosome fusion in cultured macrophages by sulfatides of *Mycobacterium tuberculosis*. *Proc. Natl. Acad. Sci. U.S.A. 73*, 2510–2514.

(9) Zhang, L., English, D., and Andersen, B. R. (1991) Activation of human neutrophils by *Mycobacterium tuberculosis*-derived sulfolipid I. *J. Immunol. 146*, 2730–2736.

(10) Zhang, L., Goren, M. B., Holzer, T. J., and Andersen, B. R. (1988) Effect of *Mycobacterium tuberculosis*-derived sulfolipid I on human phagocytic cells. *Infect. Immun. 56*, 2876–2883.

(11) Gilleron, M., Stenger, S., Mazorra, Z., Wittke, F., Mariotti, S., Böhmer, G., Prandi, J., Mori, L., Puzo, G., and De Libero, G. (2004) Diacylated sulfoglycolipids are novel mycobacterial antigens stimulating CD1-restricted T cells during infection with *Mycobacterium tuberculosis*. *J. Exp. Med. 199*, 649–659.

(12) Mougous, J. D., Leavell, M. D., Senaratne, R. H., Leigh, C. D., Williams, S. J., Riley, L. W., Leary, J. A., and Bertozzi, C. R. (2002) Discovery of sulfated metabolites in mycobacteria with a genetic and mass spectrometric approach. *Proc. Natl. Acad. Sci. U.S.A. 99*, 17037–17042.

(13) Brennan, P. J., and Goren, M. B. (1977) Mycobacterial glycolipid as bacterial antigens. *Biochem. Soc. Trans. 5*, 1687–1693.

(14) Converse, S. E., Mougous, J. D., Leavell, M. D., Leary, J. A., Bertozzi, C. R., and Cox, J. S. (2003) MmpL8 is required for sulfolipid-1 biosynthesis and *Mycobacterium tuberculosis* virulence. *Proc. Natl. Acad. Sci. U.S.A. 100*, 6121–6126.

(15) Domenech, P., Reed, M. B., Dowd, C. S., Manca, C., Kaplan, G., and Barry, C. E. III (2004) The Role of MmpL8 in Sulfatide Biogenesis and Virulence of *Mycobacterium tuberculosis*. *J. Biol. Chem. 279*, 21257–21265.

(16) Mougous, J. D., Petzold, C. J., Senaratne, R. H., Lee, D. H., Akey, D. L., Lin, F. L., Munchel, S. E., Pratt, M. R., Riley, L. W., Leary, J. A., Berger, J. M., and Bertozzi, C. R. (2004) Identification, function and structure of the mycobacterial sulfotransferase that initiates sulfolipid-1 biosynthesis. *Nat. Struct. Mol. Biol. 11*, 721–729.

(17) Sirakova, T. D., Thirumala, A. K., Dubey, V. S., Sprecher, H., and Kolattukudy, P. E. (2001) The *Mycobacterium tuberculosis* pks2 Gene Encodes the Synthase for the Hepta- and Octamethyl-branched Fatty Acids Required for Sulfolipid Synthesis. *J. Biol. Chem. 276*, 16833−16839.

(18) Mougous, J. D., Senaratne, R. H., Petzold, C. J., Jain, M., Lee, D. H., Schelle, M. W., Leavell, M. D., Cox, J. S., Leary, J. A., Riley, L. W., and Bertozzi, C. R. (2006) A sulfated metabolite produced by stf3 negatively regulates the virulence of *Mycobacterium tuberculosis*. *Proc. Natl. Acad. Sci. U.S.A. 103*, 4258−4263.

(19) Kumar, P., Schelle, M. W., Jain, M., Lin, F. L., Petzold, C. J., Leavell, M. D., Leary, J. A., Cox, J. S., and Bertozzi, C. R. (2007) PapA1 and PapA2 are acyltransferases essential for the biosynthesis of the *Mycobacterium tuberculosis* virulence factor sulfolipid-1. *Proc. Natl. Acad. Sci. U.S.A. 104*, 11221−11226.

(20) Marjanovic, O., Iavarone, A. T., and Riley, L. W. (2011) Sulfolipid accumulation in *Mycobacterium tuberculosis* disrupted in the mce2 operon. *J. Microbiol. 49*, 441−447.

(21) Layre, E., Cala-De Paepe, D., Larrouy-Maumus, G., Vaubourgeix, J., Mundayoor, S., Lindner, B., Puzo, G., and Gilleron, M. (2011) Deciphering sulfoglycolipids of *Mycobacterium tuberculosis*. *J. Lipid Res. 52*, 1098−1110.

(22) Hsu, F. F., Soehl, K., Turk, J., and Haas, A. (2011) Characterization of mycolic acids from the pathogen *Rhodococcus equi* by tandem mass spectrometry with electrospray ionization. *Anal. Biochem. 409*, 112−122.

(23) Hsu, F. F., Turk, J., Owens, R. M., Rhoades, E. R., and Russell, D. G. (2007) Structural Characterization of Phosphatidyl-myo-inositol Mannosides from *Mycobacterium bovis* Bacillus Calmette Guerin by Multiple-Stage Quadrupole Ion-Trap Mass Spectrometry with Electrospray Ionization. I. PIMs and Lyso-PIMs. *J. Am. Soc. Mass Spectrom. 18*, 466−478.

(24) Hsu, F. F., Turk, J., Owens, R. M., Rhoades, E. R., and Russell, D. G. (2007) Structural Characterization of Phosphatidyl-myo-Inositol Mannosides from *Mycobacterium bovis* Bacillus Calmette Guerin by Multiple-Stage Quadrupole Ion-Trap Mass Spectrometry with Electrospray Ionization. II. Monoacyl- and Diacyl-PIMs. *J. Am. Soc. Mass Spectrom. 18*, 479−492.